Engineered Science
DOI: https://dx.doi.org/10.30919/es960

Effect of Deep Cryogenic Treatment on Microstructure, Mechanical Properties, and Residual Stress of AISI 52100 Bearing Steel

Fuat Kara,[1,*] Adem Çiçek[2] and Halil Demir[3]

Abstract

This study covers tensile, fatigue, and material characterization tests on AISI 52100 material. In this study, the effects of deep cryogenic treatment (DCT) applied to the material at different holding hours on the mechanical properties (macro-hardness, micro-hardness, yield and tensile strength), microstructure, change in residual austenite volume ratio and residual stress values were examined. Five different holding times (12, 24, 36, 48 and 60h) were employed to the bearing steel to compare the effect of holding time in the deep cryogenic temperature. The metallographic findings showed that the deep cryogenic treatment (DCT) decreased the retained austenite and hence improved the micro-hardness, due to more homogenized carbide distribution and the elimination of the retained austenite, compared with the conventional heat treatment (CHT). The improvements in the maximum tensile strength of DCT specimens were 5.2%, 3.6%, 3.35%, 2.9% and 1.7% for DCT-36, DCT-48, DCT-60, DCT-24 and DCT-12, respectively. The highest value in macro and micro-hardness was obtained with the DCT-36 sample. It was observed that the best fatigue performance was obtained with the DCT-12 sample. In addition, the fatigue life of DCT-12, DCT-36, DCT-24, DCT-48 and DCT-60 samples increased by 122%, 108%, 100%, 40% and 12%, respectively, compared to the CHT sample. The lowest stress values for both axial and circumferential tensile residual stresses were obtained in the DCT-12 sample.

Keywords: Bearing steel, Deep cryogenic treatment, Microstructure, Residual stress, Retained austenite.
Received: 25 August 2023; Revised: 02 September 2023; Accepted: 07 September 2023.
Article type: Research article.

1. Introduction

Residue austenite and residual stresses occur in materials due to plastic deformation or thermal effects in welding, casting, forging, rolling, sheet metal forming processes, machining processes, and heat-treated materials. Residual austenite is austenite that can remain at room temperature without transforming into martensite during transformation hardening. After tempered martensite, residual austenite affects the mechanical properties of heat-treated parts the most.[1,2] If the residual austenite content is high in the structure, the hardness, wear resistance, and fatigue strength of the materials decrease. Since it affects the mechanical properties negatively, the amount of residual austenite should be reduced as much as possible in different material groups such as cementation, tool, mold, and bearing steels. At the same time, residual stresses occur in materials mainly due to mechanical, thermal, and chemical factors.[3] Mechanical factors are generally caused by non-uniform plastic deformations that occur during manufacturing. These may be deformations arising from the nature of the manufacturing process and from different manufacturing processes such as welding, machining, forging, rolling, and sandblasting.[3] Residual stresses caused by thermal factors also occur due to uneven heating and cooling conditions that occur during production or heat treatment processes.[4] On the other hand, chemical factors are based on many reasons, such as volume changes, phase transformations, chemical surface treatments, and coating processes resulting from chemical reactions.[5] Small changes in residual stresses can be critical to the life of a part. To understand the importance of these effects on parts such as bearings and gears and to evaluate the material's performance, it is necessary to know the residual stress level in part.

[1] *Department of Mechanical Engineering, Duzce University, Duzce 81620, Turkey.*
[2] *Department of Mechanical Engineering, Ankara Yıldırım Beyazıt University, Ankara 06010, Turkey.*
[3] *Department of Manufacturing Engineering, Karabük University, Karabük 78050, Turkey.*
**Email: fuatkara@duzce.edu.tr* (F. Kara)

AISI 52100 bearing steel is generally known for its use in applications requiring high fatigue and wear resistance, with high strength under cyclic loads. AISI 52100 steel; in lever taps, milling cutters, shafts, precision instrument parts, bushings, bearings, bearing rings and balls, stamping tools, gears, dies, gauges, pins, shrink disks, screws, machine and pump parts, rollers, cylinder liners and It is a type of material that is widely used in hydraulic equipment parts.[6] Therefore, this material should have high hardness, high elasticity limit, and high fatigue life. It is stated in the literature that the cryogenic treatment applied to the material after heat treatment provides significant improvements in the mechanical properties of different types of materials.[7,8] However, the number of studies revealing the effects of cryogenic treatment applied to AISI 52100 bearing steel material, which is used in manufacturing applications where wear and fatigue are important, such as bearings, on mechanical behavior, is almost non-existent. For this purpose, it aims to achieve positive improvements in the material's mechanical properties by applying deep cryogenic treatment to the AISI 52100 bearing steel material at different holding hours. Thus, by improving the material's mechanical properties, it is foreseen to increase the life of the bearings, which are of great importance in the industry, and thus reduce their high costs.

This study aims to determine the changes in mechanical properties such as hardness, tensile strength, and fatigue strength of AISI 52100 bearing steel, which is subjected to deep cryogenic treatment at different holding times (0, 12, 24, 36, 48, 60 hours). In addition, the effects of deep cryogenic treatment on residual austenite volume fraction and residual stress were investigated. However, another aim is to determine the holding time for the AISI 52100 bearing steel from the deep cryogenic treatment applied to the test sample at different holding times.

2. Material and method

This study performed two tests, tensile and fatigue, for deep cryogenic treated and untreated samples. In addition, metallographic examination, hardness, and characterization tests were performed, and changes in microstructure, macro-hardness, micro-hardness, residual austenite and residual stresses were investigated. Hardened (62 HRc) AISI 52100 bearing steel was used as test material. The chemical composition of the test sample is given in Table 1.

Table 1. Chemical composition (%) of AISI 52100 bearing steel.

C	Si	Mn	P	S	Cr	Mo	Al	Fe
0.973	0.27	0.33	0.016	0.001	1.41	0.02	0.025	Remaining

Two different combinations were obtained by applying conventional heat treatment and conventional heat treatment + cryogenic treatment + tempering treatment to the test samples. The heat and cryogenic treatment processes of the test samples are given in Fig. 1.

Fatigue tests were carried out with a (Wöhler) fatigue test device applying rotating bending stress according to ASTM E-466 and 468 (ASTM, 1982, ASTM, 1983). For each determined load value, the fatigue test was repeated five times, and the S-N (Wöhler) diagram was created by taking the average number of cycles during rupture. The study created fatigue graphs (Wöhler S-N diagrams) according to ASTM E 739. Equation 1 was used while determining the fatigue strength value.

$$\sigma = 10{,}18\frac{L.F}{d^3} \quad (1)$$

Here, σ: Maximum stress acting on the sample (MPa)
L: Length of the bar (mm)
F: Load (N)
d: Diameter (mm).

In the tensile tests, the tensile speed was taken as 1 mm/min. Micro-hardness was measured using SHIMADZU HMW (ASTM E-18) micro-hardness tester. The dimensions of micro-hardness samples were Ø10x10 mm. On each sample, up to 10 hardness measurements were performed across the surface in order to obtain representative average hardness values. All hardness tests were carried out at room temperature. The microstructures were characterized by LEO 1430 VP scanning electron microscope (SEM). The phase analysis and volume fraction of retained austenite was determined using the SEIFERT Analytical X-ray MZ VI diffraction instrument with Cr Kα X-ray source.

3. Results and discussion

3.1 Microstructural evaluation

In the cryogenic treatment, to optimize the metallurgical aspects by material to be treated under freezing low temperature for a predetermined period to obtain the crystalline metallurgical structure of the material to improve the hardness, strength, ductility, toughness, resistance, etc., and to a reduction in residual stresses, which enhances the stability during the machining.[9] In recent years, different hypotheses have been reported about microstructure observations in the literature. One of these to increase the percentage of carbide in microstructure of materials after the deep cryogenic treatment. The reason is martensite and austenite lattice contraction; the chromium carbide distribution was more homogenized after the deep cryogenic treatment. Because of this shrinkage, carbon atoms are forced to diffuse and make a new carbide nucleus. This new carbide nucleus increases the carbide percentage and the homogenous distribution.[10] The cryogenic treatment had a significant effect on the alloy's microstructure and led to the transformation of retained austenite to martensite. As the cryogenic temperature is lowered, more austenite is transformed into martensite.[11] In this study, microstructural examinations were performed to determine caused by changes in microstructure of deep cryogenic treatment carried out in different holding times. The microstructures of AISI 52100

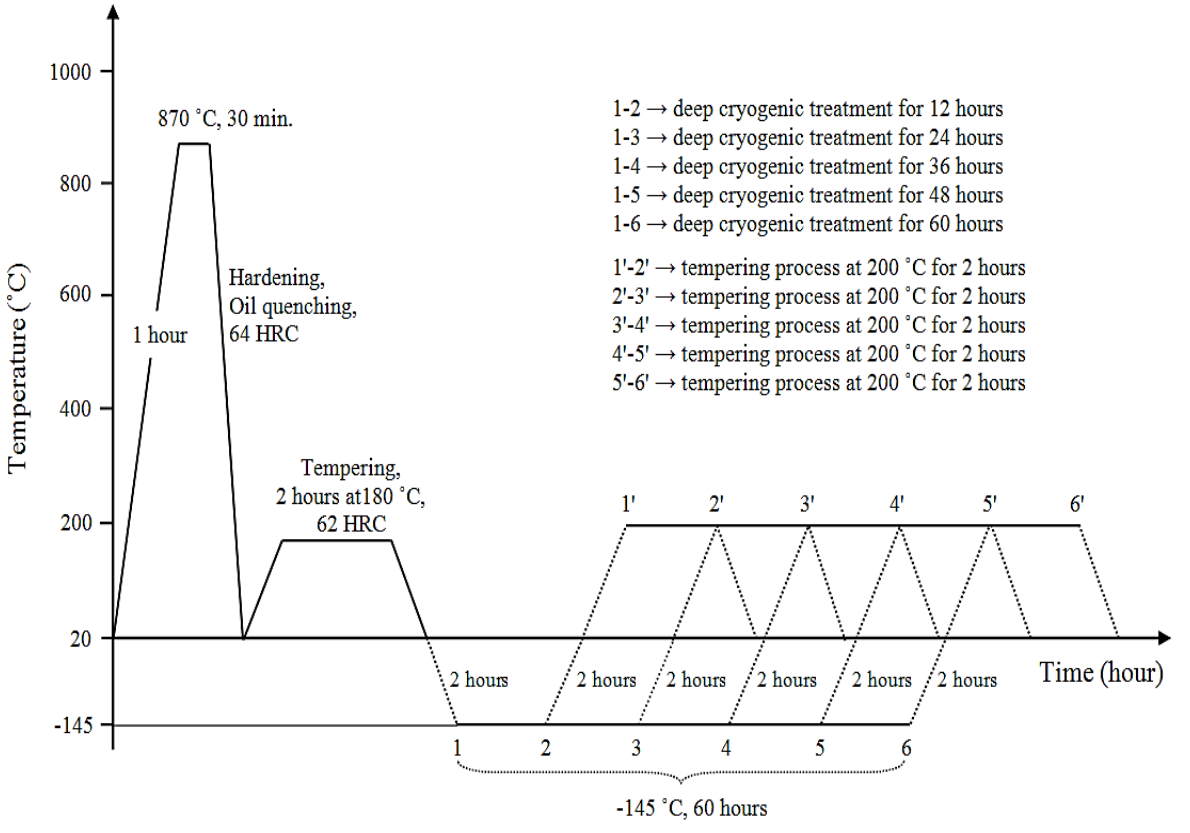

Fig. 1 Heat treatment curve of AISI 52100 steel.

bearing steel samples, deep cryogenically treated and conventional heat treated, are shown in Figs. 2(a-f). In Fig. 2, CHT samples exhibited a non-uniform chromium carbides distribution, while DCT samples exhibited uniform distribution of white regions of primary chromium carbides and nearly spherical secondary chromium carbides. Also, the microstructure images showed that the carbide percentage increased in the DCT samples compared with CHT samples. In addition, it was performed that smaller carbide size and more uniform carbide distribution were formed after the deep cryogenic treatment. This improvement is a consequence of the retained austenite elimination that transformation of retained austenite to martensite. Besides, it may be explained that the secondary carbides precipitate in the austenite matrix, causing shrinkage of carbide particles and more homogeneous carbide distribution with a tempering process performed after deep cryogenic treatment.

Four main metallurgical aspects explain the changes in the properties of cryo-processed materials: the transformation of retained austenite to martensite, formation of eta (h)–carbides, precipitation of ultrafine carbides, homogeneous microstructure.[9] One of these the transformation of retained austenite to martensite. The retained austenite as a soft phase in steels could reduce the product life, and, in working conditions, it can be transformed into martensite. Changes in the percentages of retained austenite in microstructure of AISI 52100 bearing steel after DCT are given in Table 2. As can be seen clearly from the table, the deep cryogenic process reduced the percentage of retained austenite in the bearing steel. This reduction was performed as per cent 20, 37, 51, 46 and 40 for DCT-12, DCT-24, DCT-36, DCT-48 and DCT-60, respectively. The measurement of the percentage of retained austenite in the microstructure (Table 2) also verified the transformation of retained austenite to martensite.

Figure 3 shows the X-ray diffraction pattern of the CHT and the DCT samples. The peaks corresponding to martensite retained austenite, and carbides are visible. After DCT, the peaks of austenite have a low-intensity value due to the transformation of retained austenite to martensite during the DCT. The maximum transformation of austenite was performed DCT-36 sample. This result was confirmed by the microstructure images and measurements of retained austenite. The measurement of the XRD pattern also indicates that the retained austenite has transformed into martensite during DCT.

Table 2. Retained austenite volume content after different treatment cycles.

Sample	CHT	DCT-12	DCT-24	DCT-36	DCT-48	DCT-60
Retained austenite percent (%)	7.0	5.6	4.4	3.4	3.8	4.2

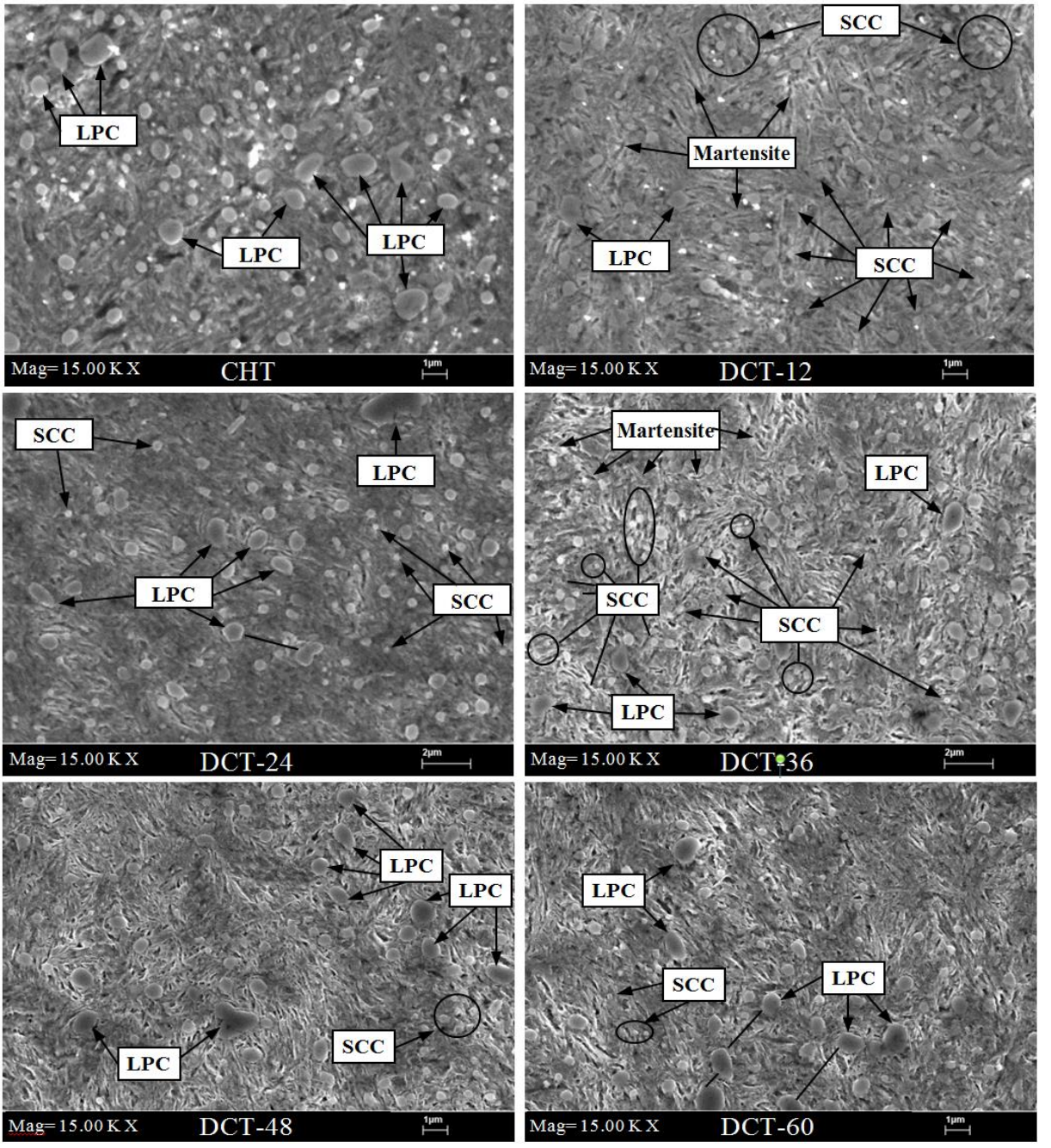

Fig. 2 Microstructure of the bearing steel samples (LPC-large primary carbide, SCC-small secondary carbide).

3.2 Evaluation of hardness and tensile behaviors

During deep cryogenic treatment, the secondary carbides precipitate in the austenite matrix, promote the transformation of the retained austenite to martensite and consequently enhance hardness of the alloy.[12,13] The measurement of hardness and tensile tests of differently heat-treated specimens are shown in Table 3. The Vickers hardness values for CHT, DCT-12, DCT-24, DCT-36, DCT-48 and DCT-60 specimens are 740, 757, 770, 802, 788 and 782 HV, respectively. The DCT samples have a higher hardness compared with the CHT samples. Also, the highest hardness value was measured in the sample, which was cryo-treated for 36 h. It may be attributed to the completion of phase transformation in this holding time. The higher hardness of the DCT samples was due to the decrease in retained austenite. Also, the DCT samples retained austenite elimination, had a more homogenized chromium carbide distribution, and increased hardness due to the higher chromium carbide percentage. In addition, the higher martensite contents and carbon percentages increase the hardness of steel. Consequently, the micro-hardness results shown that the deep cryogenic treatment improved the hardness of the bearing steel samples for 10% compared with conventional heat treatment. The change in macro-hardness values showed parallelism with micro-hardness. When the DCT samples were compared among themselves, the highest macro-hardness values were obtained with the DCT-36 sample, as in the micro-hardness measurement results.

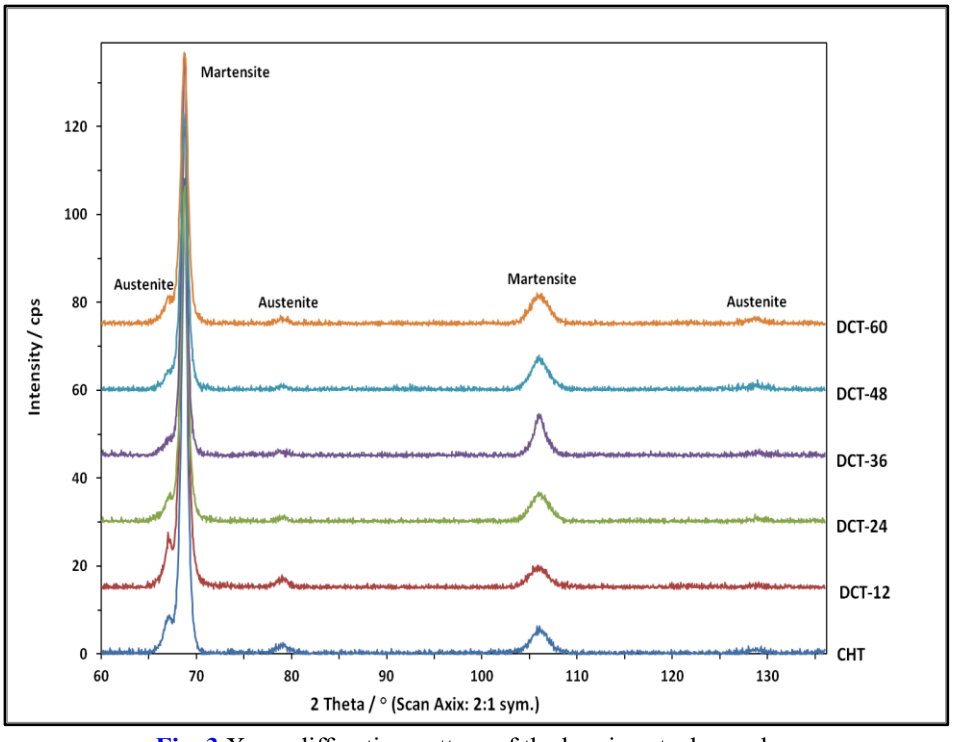

Fig. 3 X-ray diffraction pattern of the bearing steel samples.

Table 3. Results of tensile tests at room temperature for AISI 52100 bearing steel.

Materials	Yield strength (MPa)	Maximum n tensile strength (MPa)	Elongation (%)	Macro-hardness (HRC)	Micro-hardness ($HV_{0.1}$)
CHT	1824	2218	4.46	62	740
DCT-12	1840	2256	3.93	62.3	757
DCT-24	1851	2283	3.84	62.9	770
DCT-36	1880	2334	2.39	64	802
DCT-48	1872	2298	2.63	63.6	788
DCT-60	1863	2292	2.82	63.2	782

When we look at the yield and maximum tensile strength results in Table 3, it is seen that the highest values are in DCT-36, DCT-48, DCT-60, DCT-24, DCT-12, and CHT samples, respectively. As can be seen from the tensile test results, the yield and tensile strengths of the bearing steel samples, which were subjected to deep cryogenic treatment, were found to be higher when compared to the conventional heat-treated samples. Improvements in yield strength of deep cryogenically treated specimens were 3.1%, 2.6%, 2.1%, 1.5% and 1.5% for DCT-36, DCT-48, DCT-60, DCT-24 and DCT-12, respectively. It was found to be 0.9. However, the improvements in the maximum tensile strength of DKI specimens were 5.2%, 3.6%, 3.35%, 2.9% for DCT-36, DCT-48, DCT-60, DCT-24 and DCT-12, respectively. It was found to be 1.7%. Among the deep cryogenically treated samples, the highest yield and tensile stress values were obtained with the DCT-36 sample. This result was associated with a higher rate of austenite-martensite transformation in the material's microstructure with deep cryogenic treatment in DCT-36 samples than in other DCT samples. Phase analyzes and residual austenite volume fraction calculations also confirmed this result. In addition, it has been reported in literature studies that mechanical properties improve after cryogenic treatment. Bensely *et al.* (2007) found an improvement of 9.34% in the tensile strength of samples that were cryogenically treated for 24 hours at -196 °C.[14] In another study, Koneshlou *et al.* (2011) stated that after deep cryogenic treatment, the residual austenite volume ratio decreased from 8.1% to 3.8%, and the tensile strength was improved by 8.9%.[9] In this context, it is possible to say that the results of the tensile test are parallel with the results of the literature. When we look at the elongation values, it is seen that the lowest values are in DCT-36, DCT-60, DCT-48, DCT-24, DCT-12, and CHT samples, respectively. This can be explained by the fact that the elongation value changes inversely to the yield and tensile stresses, which is related to the ductility or brittleness of the materials.

Figure 4 shows SEM images of the fracture surfaces of six different samples according to the treatment type. Fractured surface photographs showed both ductile and brittle fracture mechanisms in the samples. The first point that draws attention here is that the ruptured surface of the CHT sample is rougher and indented than the other samples. These jagged surface images are also known as step-like structures. Step structures

are generally located away from the crack initiation point where micro-voids and pits are not observed.[15] Step structures are usually associated with a vein-like structure. They are also referred to as "river patterns" and are often observed on fractured surfaces of amorphous metals.[16] The vein-like surface conditions that cause stepper structures are associated with the formation of liquid-like low-viscosity layers that form on the slip band during plastic deformation. The entire fractured surface of the CHT sample was covered with step-like structures. Although the step-like formation may appear for the CHT sample, these structures are not steppe formations because the steps are very irregular. The CHT sample has rapid and irregular crack propagation following intergranular fracture. It was observed that the CHT sample exhibited a ductile fracture mechanism, while the deep cryogenically treated samples exhibited a brittle fracture mechanism. In steels, ductility generally decreases with increasing hardness.[14,17-20] Matrix hardness increases with increasing cryogenic treatment retention time, and this increase causes a decrease in the degree of plasticity. Low plasticity or plastic deformation leads to the formation of micro-pits and rapid crack propagation. In this case, the matrix with increased hardness causes damage without showing plastic deformation, as in cast iron.

Another point to be considered in DCT samples is that the formation of a fine carbide structure due to the deep cryogenic treatment retention time causes the fractured surface to appear flat. In this case, as a result of increased hardness, the plasticity of the sample decreases, and the formation of a pit indicating ductile rupture causes an volumetric reduction. If we compare the DCT samples with each other, it can be said that the surface images are generally similar in all DCT samples. Still, only the DCT-12 and DCT-36 samples exhibit more brittle fracture behavior than the others, and the fracture event occurs. In the studies conducted, it has been stated that the ductile structure of the materials decreases after the cryogenic treatment and they fracture by exhibiting a more brittle fracture mechanism.[9,11,14] Bensely *et al.* (2007) studied the change in fracture surfaces of carburized 815M17 steel after deep cryogenic treatment. While ductile pits and flat surfaces showing brittleness were found on the fractured surfaces of the conventional heat-treated sample, it was observed that the brittle pits and flat surfaces showing brittleness increased in the deep cryogenically treated samples. In addition, the presence of mixed mode with ductile and brittle fracture mechanisms was detected in all samples.[11]

In the 1000X magnification SEM images, macro and micro-cracks formed on the fracture surfaces of six different samples are seen. In the tensile test, when the breaking point is approached, cracks begin to form on the sample surfaces with the effect of plastic deformation. Depending on the ductility of the materials, the samples with cracks on the surface break for specific periods. These cracks can be clearly seen when the surfaces of the material subject to permanent deformation are examined. If we evaluate the cracks formed on the sample surfaces according to the treatment type, it is seen that the largest cracks are in the conventional heat-treated CHT sample. Micro-cracks were formed in DCT-24, DCT-48, and DCT-60 samples, while no apparent cracks were observed in DCT-12 and DCT-36 samples. Since the material has a more brittle structure with the deep cryogenic process, the cracks formed during rupture occurred in micro sizes, smaller than the CHT sample.

When looking at the SEM images at 5000X magnification, it is seen that there are pits and voids along with cracks on the surfaces of all samples. The size or smallness of the pits on the sample surface is an indication that the material has a ductile or brittle structure. It is seen that there are large pits and voids on the fractured surfaces of the CHT sample. However, the pits and voids formed on the surface of the CHT sample are larger and more numerous than the other two samples, both in size and in number. The pits and cavities that are widely distributed on the fracture surface prove that the specimen was subjected to plastic deformation to a large extent before the fracture.[14] The structure shown in the figure is a feature specific to the fracture surface formed by uniaxial tensile stress. Each pit in the figure is half of a micro-void that was formed earlier and then separated by fracture.[21] The dimple-shaped pits on the surfaces of the samples differ according to the type of treatment. The pits on the surface of the CHT sample are larger, deeper and ductile. The structure of these pits is ductile. However, the distribution of pits on the surface of this sample is not homogeneous due to the abundance of cracks on the surface.

On the other hand, the pits on the surfaces of DCT samples are more homogeneously distributed and have a shallower structure. Das *et al.* (2010), in their study examining the fractured surfaces of AISI D2 cold work tool steel, determined that the number of pits on the fractured surfaces of the deep cryogenically treated samples increased, and the pits had a shallower structure compared to the conventional heat-treated samples. They associated this with improved mechanical properties after cryogenic treatment and less plastic deformation of the samples.[9]

Another striking point in Fig. 4 is the increase in the area and number of flat surfaces showing the brittle structure on the fractured surfaces of the samples after deep cryogenic processing. While it is seen that there are very few flat surfaces on the fractured surfaces of the conventional heat-treated sample, it is observed that these formations increase significantly in all the fractured surfaces of the DCT samples. With the increase of these flat surface formations, the ductility of the DCT samples decreased and turned into a more brittle structure. The obtained hardness measurements and tensile test results also supported this situation.

3.3. Evaluation of residual stress

Residual stresses are the stresses remaining in part as a result of various manufacturing processes, heat treatment processes, or inhomogeneous deformation of the materials. Since

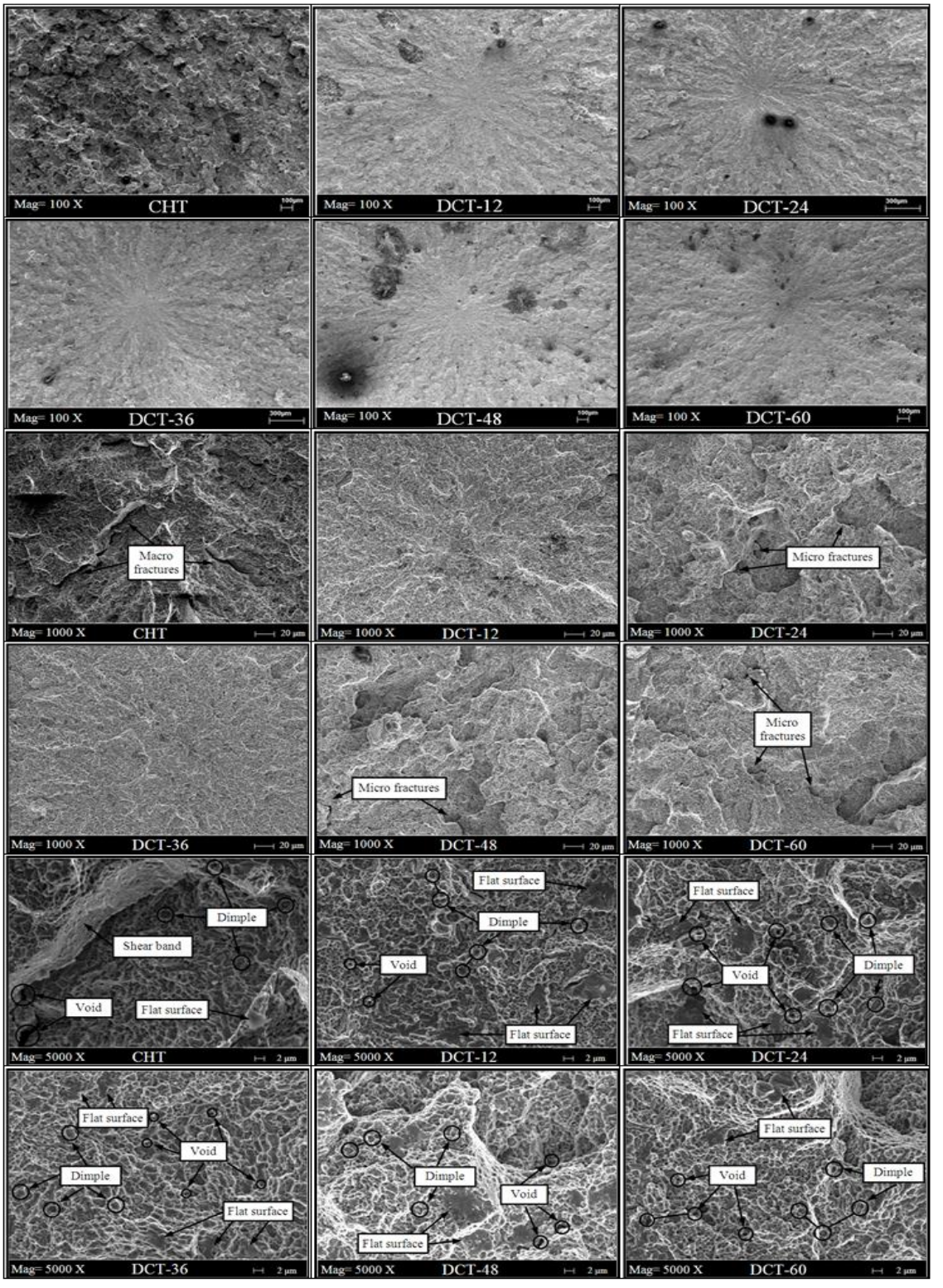

Fig. 4 Fracture surfaces of tensile specimens.

residual stresses remain in part after production, external loads and forces during use affect the part with these stresses.[22] Residual stresses directly affect the working life of the produced material.[23] Compressive residual stress generally benefits fatigue life and corrosion resistance as it retards crack initiation and growth. On the contrary, tensile residual stress reduces the mechanical performance of materials.[22,24] The axial and circumferential residual stress values measured in the samples after conventional heat treatment and deep cryogenic treatment are given in Figs. 5 and 6. In Fig. 5, axial residual stress values varied between 50 MPa and 170 MPa. While the highest axial tensile residual stress was obtained in DCT-48 sample at 25 µm depth, 173 MPa, the lowest stress value was obtained as 54.9 MPa in DCT-12 sample at 150µm depth. In Fig. 6, circumferential residual stress values varied between 35 MPa and 180 MPa. While the highest peripheral

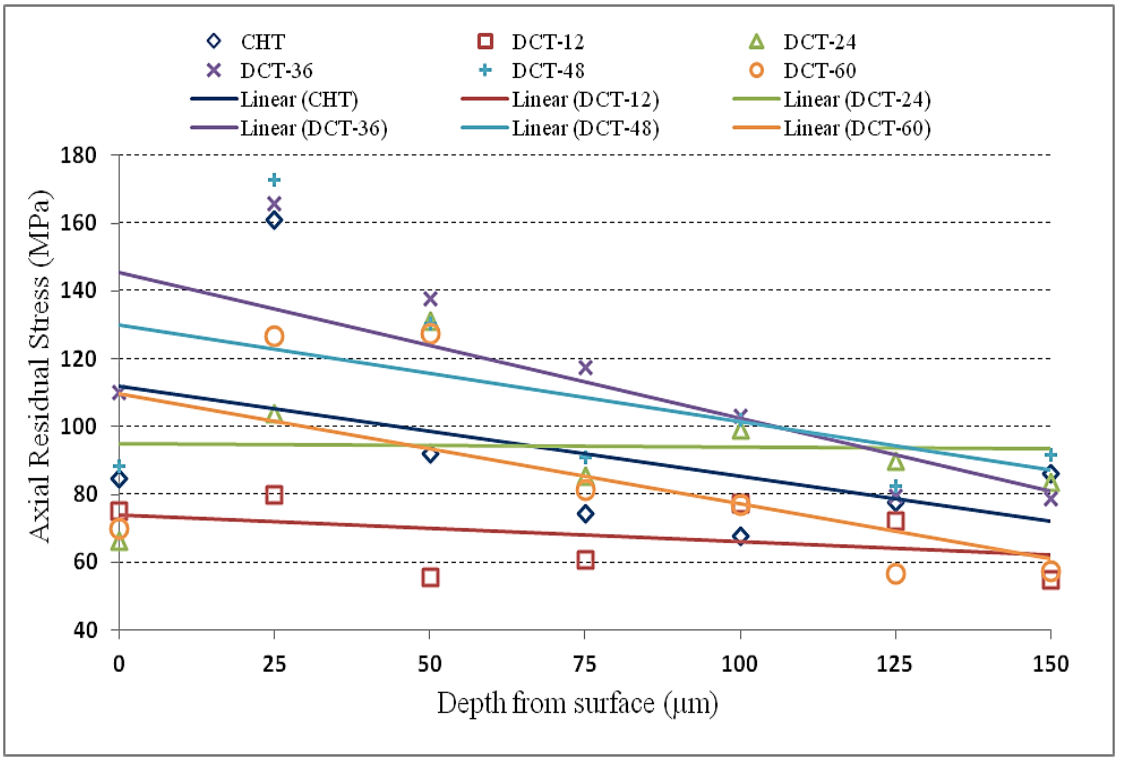

Fig. 5 Variation of axial residual stresses.

tensile residual stress was obtained in the conventional heat-treated CHT sample at 25 µm depth, 180 MPa, the lowest stress value was obtained as 36.4 MPa in the DCT-12 sample at 75 µm depth. When we look at Fig. 5 and Fig. 6, it is seen that tensile residual stresses occur at the surface and near the surface for all samples, while tensile residual stresses decrease with the increase in depth with the effect of residual stresses in the compression direction.

As can be seen from both figures, the lowest stress values for both axial and circumferential tensile residual stresses were obtained in the DCT-12 sample. This result confirmed that, as stated in the literature,[25-27] deep cryogenic treatment reduces tensile residual stresses by creating stresses in the compression direction. Bensely *et al.* (2008) obtained the residual stress values before tempering as -125 MPa, -115 MPa, and -235 MPa for conventional heat-treated, shallow cryogenic treated, and deep cryogenic-treated samples, respectively. On the other hand, the residual stress values after tempering were found as -150 MPa, -80 MPa, and -80 MPa for conventional heat-treated, shallow cryogenic treated, and deep cryogenic treated samples, respectively.[28] Jung *et al.* (1996) stated in their study that the compressive residual stresses

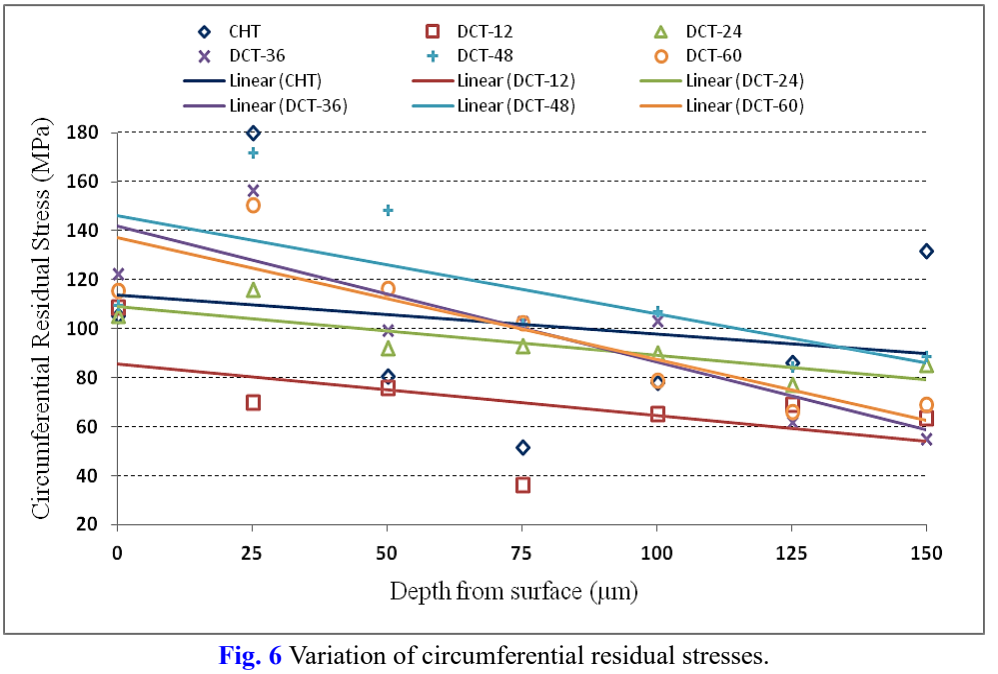

Fig. 6 Variation of circumferential residual stresses.

in AISI 4320 and AISI 9310 steels increased after shallow and deep cryogenic processing. Recovery in residual stresses has been associated with the conversion of residual austenite to martensite during shallow and deep cryogenic processing.[29] Sentilkumar *et al.* (2011) concluded that the maximum residual compressive stresses occur after deep cryogenic treatment and before tempering. They stated that residual stresses occur due to the load and thermal changes exposed to the workpiece.[25]

These studies' results indicate that cooling metals below room temperature plays an important role in terms of residual stress. The substantial stress relief in the tempered deep cryogenic treatment samples may be due to the formation of finer precipitations throughout the matrix and the loss of tetragonality of the martensite. Also, the mechanism behind the large variation in residual stresses may be due to atomic level changes that occur during the tempering process as well as the deep cryogenic processes of cooling, holding, and heating to room temperature. The cooling step, which is the first of the deep cryogenic processing processes, causes the residual austenite to transform into newly formed martensite, which has different lattice parameters (higher c/a ratio) than the original martensite.[30] Villa *et al.* (2012) measured lattice parameters a, 2.861Å and c, 2.960Å for the conventional heat-treated sample, while a, 2.859Å and c, 2.967Å after cryogenic treatment. Thus, the average c/a ratio of the samples, namely the tetragonality, increased from 1.035 to 1.038.[31] This significant increase in tetragonality was explained by the decrease in the tetragonality of martensite and the formation of carbon aggregation in the lattice defects during prolonged room temperature storage for the first case.[32]

Another point that draws attention from both graphs is that the tensile residual stresses start to rise after this holding time, during which the tensile residual stresses decrease with the cryogenic process for up to 12 hours. These results showed parallelism with the results of the study by Yong and Ding (2011). After cryogenic treatment, Yong and Ding (2011) investigated residual stress changes in WC-Co cemented carbides. The residual stresses were measured as -496, -1459, and -1391 MPa in conventional heat treated, 2-hour cryogenic treated, and 24-hour cryogenic treated samples, respectively. The authors explained the large changes in residual stresses, as mentioned above, with the atomic level changes during the cryogenic process and the different behavior of the lattice parameters “a” and “c” during cooling and heating.[33] Figs. 5 and 6 show that considering the average of the axial and circumferential tensile residual stress values at all surface depths, the lowest stress values were obtained in the DCT-12 sample for both axial residual stresses and peripheral residual stresses. Based on these results, it can be said that 12 hours is the ideal holding time for deep cryogenically treated AISI 52100 bearing steel in terms of residual stress formation. Residual stresses are the most effective on fatigue strength among the mechanical properties of materials.[34,35] When an evaluation is made in this context, It has been seen that the residual stress results and the fatigue test results are in parallel, and the best results for both cases are obtained with the DCT-12 sample.

3.4. Evaluation of fatigue life

Figure 7 shows the changes in the number of cycles at different stresses of deep cryogenically treated bearing steels at different residence times. In literature studies in which the Wöhler curve was created, 10^7 cycles were determined as the fatigue limit.[36] Fatigue tests were completed when 10^7 cycles were reached. The fatigue limit for all samples was reached with a stress value of 850 MPa, as in the literature studies on the fatigue performance of AISI 52100 bearing steel.[37,38] In order to better detect the difference in the deep cryogenic process, only the Wöhler curve of the CHT sample was created in the graph. When we look at the graph, it is understood that the cycle numbers of the deep cryogenically treated samples are generally on the right of the curve; that is, they break in a longer lifetime than the CHT sample. This result was associated with the increase in fatigue strength of the materials by cryogenic treatment, as stated in the studies in the literature. Zhirafar *et al.* (2007), in their study on the mechanical properties of AISI 4340 steel, concluded that the fatigue limit of the steel improved after cryogenic treatment and tempering.[39] In another study, Singh *et al.* (2005) provided a 100% improvement in fatigue life after cryogenic treatment.[26] Residual austenite in the structure of the steel; adversely affects steel properties by reducing yield, tensile, fatigue strength, and compressive residual stresses. With the cryogenic treatment of steels under the same conditions, this residual austenite, which remains in the structure, turns into martensite, causing an increase in fatigue strength.[1] Baldissera (2009) determined that the fatigue strength of the cryogenically treated samples increased. Baldissera associated this improvement in fatigue strength with fine carbide precipitation in the microstructure after cryogenic treatment, conversion of residual austenite to martensite, and residual stress changes.[40]

When a general evaluation is made by taking the average of the number of cycles obtained at 900, 950, and 1000 MPa stress values for all samples, it is seen that the best fatigue performance is obtained with the DCT-12 sample. In addition, the fatigue life of DCT-12, DCT-36, DCT-24, DCT-48 and DCT-60 samples increased by 122%, 108%, 100%, 40% and 12%, respectively, compared to the CHT sample. Obtaining the best fatigue behaviors in the DCT-12 sample was associated with two conditions, the residual austenite volume ratio and the residual stress values measured in this sample.

5. Conclusions

In this study, the effects of deep cryogenic treatment (-145 °C) applied at different holding times (12, 24, 36, 48 and 60 hours) on the microstructure, residual austenite volume fraction, residual stress values, fatigue strength and mechanical properties of AISI 52100 bearing steel has been researched.

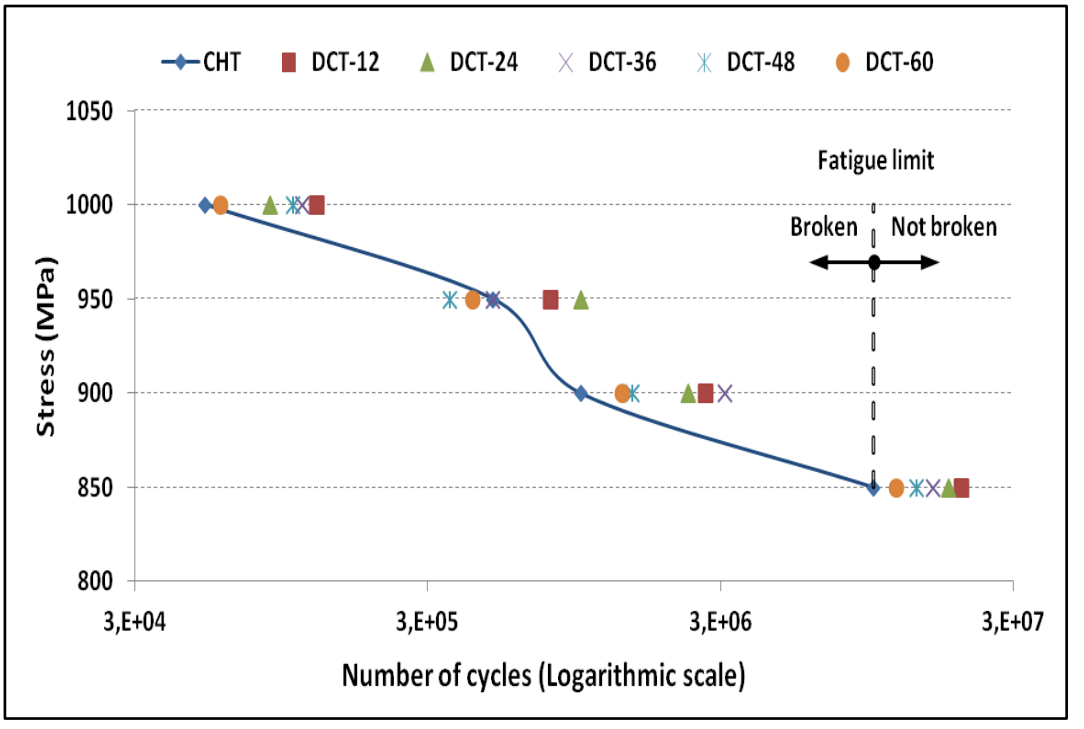

Fig. 7 Variation in fatigue life according to heat treatment type.

Obtained results are listed below.

- In the micro-hardness and macro-hardness measurements, the hardness values of the deep cryogenically treated DCT samples were greater than the untreated CHT sample. The highest hardness value among DCT samples was obtained with DCT-36 sample. These results were associated with the transformation of the soft austenite phase in the material's microstructure into martensite, which has a hard structure, together with the deep cryogenic treatment.
- When the fracture surfaces of the samples were examined after the tensile test, it was observed that the fracture surface of the conventional heat-treated CHT sample had a rougher and more distorted structure than the fracture surfaces of the DCT samples. This was attributed to the CHT sample's lower yield strength and greater plastic deformation.
- The lowest tensile residual stresses for both axial and circumferential-tangential residual stresses were measured in the DCT-12 specimen. These results revealed that deep cryogenic treatment generally reduces unwanted tensile residual stresses in materials.
- In fatigue tests, the DCT-12 sample showed the best performance, with an improvement of 122% when compared to the conventional heat-treated sample in terms of fatigue strength. Afterward, it was observed that the fatigue strengths of DCT-36, DCT-24, DCT-48, DCT-60, and CHT samples improved by 108%, 100%, 40%, and 12%, respectively. Residual stress measurements confirmed the fatigue test results based on the knowledge that tensile residual stresses adversely affect fatigue strength.
- When microstructural analyses were examined, DCT-36 sample exhibited the best microstructural properties with more homogeneous microstructure and finer carbide precipitation.
- In the residual austenite volume ratio measurements, the lowest and highest austenite volume ratios were obtained with DCT-36 and CHT samples. Considering the phase analyses performed to confirm the change in residual austenite volume ratios, the most austenite-martensite transformation was observed in DCT-36 sample.

Consequently, DCT demonstrated more improvement in the hardness, tensile strength, residual austenite, residual stress, and fatigue life than CHT.

Acknowledgments

The authors wish to place their sincere thanks to Karabük University Scientific Research Project Division for financial support for the Project No: KBÜ-BAP-11/2-DR-003.

Conflict of Interest

There is no conflict of interest.

Supporting Information

Not applicable.

References

[1] G. Parish, Carburizing: Microstructures and Properties, ASM International, Metals Park OH, 1999.

[2] Tianyi, Zhang, Effects of TiC and residual austenite synergistic strengthening mechanism on impact-abrasive wear behavior of bainite steel, *Wear*, 2021, **486-487**, 204088, doi: 10.1016/j.wear.2021.204088.

[3] S. Spor, N. Jäger, M. Meindlhumer, H. Hruby, M. Burghammer, F. Nahif, C. Mitterer, J. Keckes, R. Daniel, Evolution of structure, residual stress, thermal stability and wear resistance of nanocrystalline multilayered $Al_{0.7}Cr_{0.3}N$-

$Al_{0.67}Ti_{0.33}N$ coatings, *Surface and Coatings Technology*, 2021, **425**, 127712, doi: 10.1016/j.surfcoat.2021.127712.
[4] R. C. McClung, A literature survey on the stability and significance of residual stresses during fatigue, *Fatigue & Fracture of Engineering Materials & Structures*, 2007, **30**, 173-205, doi: 10.1111/j.1460-2695.2007.01102.x.
[5] N. Hrabe, T. Gnäupel-Herold, T. Quinn, Fatigue properties of a titanium alloy (Ti-6Al-4V) fabricated via electron beam melting (EBM): effectss of internal defects and residual stress, *International Journal of Fatigue*, 2017, **94**, 202-210, doi: 10.1016/j.ijfatigue.2016.04.022.
[6] A. Panda, A. K. Sahoo, R. Kumar, R. K. Das, A review on machinability aspects for AISI 52100 bearing steel, *Materials Today: Proceedings*, 2020, **23**, 617-621, doi: 10.1016/j.matpr.2019.05.422.
[7] O. Özbek, Effects of deep cryogenic treatment with different holding times on the mechanical properties of Al_{7050}-T7451 alloy friction stir welding, *Materials Testing*, 2023, **65**, 364-377, doi: 10.1515/mt-2022-0277.
[8] F. Kara, Y. Küçük, O. Özbek, N. Altan Özbek, M. S. Gök, E. Altaş, İ. Uygur, Effect of cryogenic treatment on wear behavior of Sleipner cold work tool steel, *Tribology International*, 2023, **180**, 108301, doi: 10.1016/j.triboint.2023.108301.
[9] D. Das, A. K. Dutta, K. K. Ray, Sub-zero treatments of AISI D2 steel: part I. Microstructure and hardness, *Materials Science and Engineering: A*, 2010, **527**, 2182-2193, doi: 10.1016/j.msea.2009.10.070.
[10] S. Li, Y. Xie, X. Wu, Hardness and toughness investigations of deep cryogenic treated cold work Die steel, *Cryogenics*, 2010, **50**, 89-92, doi: 10.1016/j.cryogenics.2009.12.005.
[11] M. Koneshlou, K. Meshinchi Asl, F. Khomamizadeh, Effect of cryogenic treatment on microstructure, mechanical and wear behaviors of AISI H13 hot work tool steel, *Cryogenics*, 2011, **51**, 55-61, doi: 10.1016/j.cryogenics.2010.11.001.
[12] V. Firouzdor, E. Nejati, F. Khomamizadeh, Effect of deep cryogenic treatment on wear resistance and tool life of M2 HSS drill, *Journal of Materials Processing Technology*, 2008, **206**, 467-472, doi: 10.1016/j.jmatprotec.2007.12.072.
[13] N. Altan Özbek, O. Özbek, Effect of cryogenic treatment holding time on mechanical and microstructural properties of Sverker 21 steel, *Materials Testing*, 2022, **64**, 1809-1817, doi: 10.1515/mt-2022-0207.
[14] A. Bensely, D. Senthilkumar, D. Mohan Lal, G. Nagarajan, A. Rajadurai, Effect of cryogenic treatment on tensile behavior of case carburized steel-815M17, *Materials Characterization*, 2007, **58**, 485-491, doi: 10.1016/j.matchar.2006.06.019.
[15] C. Wei, J. F. Yang, A finite element analysis of the effects of residual stress, substrate roughness and non-uniform stress distribution on the mechanical properties of diamond-like carbon films, *Diamond and Related Materials*, 2011, **20**, 839-844, doi: 10.1016/j.diamond.2011.04.004.
[16] F. E. Luborsky, Amorphous Metallic Alloys, Butterworths, Toronto, Canada, 1983, 231-232.
[17] M. A. Jaswin, D. M. Lal, Effect of cryogenic treatment on the tensile behaviour of En 52 and 21-4N valve steels at room and elevated temperatures, *Materials & Design*, 2011, **32**, 2429-2437, doi: 10.1016/j.matdes.2010.11.065.
[18] V. G. Gavriljuk, W. Theisen, V. V. Sirosh, E. V. Polshin, A. Kortmann, G. S. Mogilny, Y. N. Petrov, Y. V. Tarusin, Low-temperature martensitic transformation in tool steels in relation to their deep cryogenic treatment, *Acta Materialia*, 2013, **61**, 1705-1715, doi: 10.1016/j.actamat.2012.11.045.
[19] M. Koyama, T. Lee, C. S. Lee, K. Tsuzaki, Grain refinement effect on cryogenic tensile ductility in a Fe-Mn-C twinning-induced plasticity steel, *Materials & Design*, 2013, **49**, 234-241, doi: 10.1016/j.matdes.2013.01.061.
[20] V. Leskovšek, B. Podgornik, Vacuum heat treatment, deep cryogenic treatment and simultaneous pulse plasma nitriding and tempering of P/M S390MC steel, *Materials Science and Engineering: A*, 2012, **531**, 119-129, doi: 10.1016/j.msea.2011.10.044.
[21] W. D. Callister, D.G. Rethwisch, Materials Science and Engineering, John Wiley High Education, Chichester, U.K. 2010, 10-50.
[22] F. Kara, O. Özbek, N. Altan Özbek, İ. Uygur, Investigation of the effect of deep cryogenic process on residual stress and residual austenite, *Gazi Journal of Engineering Sciences*, 2021, **7**, 143-151, doi: 10.30855/gmbd.2021.02.07.
[23] Q. Sun, D. Qian, J. Liu, J. Sun, Z. Sun, Effect of deep cryogenic treatment on mechanical properties and residual stress of AlSi10Mg alloy fabricated by laser powder bed fusion, *Journal of Materials Processing Technology,* 2022, **303**, 117543, doi:10.1016/j.jmatprotec.2022.
[24] M. Biček, F. Dumont, C. Courbon, F. Pušavec, J. Rech, J. Kopač, Cryogenic machining as an alternative turning process of normalized and hardened AISI 52100 bearing steel, *Journal of Materials Processing Technology*, 2012, **212**, 2609-2618, doi: 10.1016/j.jmatprotec.2012.07.022.
[25] D. Senthilkumar, I. Rajendran, M. Pellizzari, J. Siiriainen, Influence of shallow and deep cryogenic treatment on the residual state of stress of 4140 steel, *Journal of Materials Processing Technology*, 2011, **211**, 396-401, doi: 10.1016/j.jmatprotec.2010.10.018.
[26] P. J. Singh, S. L. Mannan, T. Jayakumar, D. R. G. Achar, Fatigue life extension of notches in AISI 304L weldments using deep cryogenic treatment, *Engineering Failure Analysis*, 2005, **12**, 263-271, doi: 10.1016/j.engfailanal.2004.03.008.
[27] S. Smith, S. N. Melkote, E. Lara-Curzio, T. R. Watkins, L. Allard, L. Riester, Effect of surface integrity of hard turned AISI 52100 steel on fatigue performance, *Materials Science and Engineering: A*, 2007, **459**, 337-346, doi: 10.1016/j.msea.2007.01.011.
[28] A. Bensely, S. Venkatesh, D. Mohan Lal, G. Nagarajan, A. Rajadurai, K. Junik, Effect of cryogenic treatment on distribution of residual stress in case carburized En 353 steel, *Materials Science and Engineering: A*, 2008, **479**, 229-235, doi: 10.1016/j.msea.2007.07.035.
[29] S.-C. Jung, D. J. Medlin, G. Krauss, Effects of Subzero Treatments on the Bending Fatigue Performance of Carburized SAE-4320 and SAE-9310 SteelsSAE Technical Paper Series. 400

Commonwealth Drive, Warrendale, PA, United States: SAE International, 1996, doi: 10.4271/960313.
[30] P. L. Yen, Effect of cryogenic treatment on the wear resistance of tool steel, PhD. Thesis, The Pennsylvania State University, Pennsylvania, U.S.A., 1996.
[31] M. Villa, F. B. Grumsen, K. Pantleon, M. A. J. Somers, Martensitic transformation and stress partitioning in a high-carbon steel, *Scripta Materialia*, 2012, **67**, 621-624, doi: 10.1016/j.scriptamat.2012.06.027.
[32] L. Cheng, A. Böttger, E. J. Mittemeijer, Tempering of iron-carbon-nitrogen martensites, *Metallurgical Transactions A*, 1992, **23**, 1129-1145, doi: 10.1007/BF02665045.
[33] J. Yong, C. Ding, Effect of cryogenic treatment on WC-Co cemented carbides, *Materials Science and Engineering*: *A*, 2011, **528**, 1735-1739, doi: 10.1016/j.msea.2010.11.009.
[34] G. Totten, M. Howes, T. Inoue, Handbook of Residual Stress and Deformation of Steel, ASM International, Ohio, U.S.A. 2002, 11-26.
[35] D. Ulutan, Predictive modeling and multi–objective optimization of machining–induced residual stresses: Investigation of machining parameter effects, The State University of New Jersey, Degree of Doctor of Philosophy, New Jersey, 2013.
[36] D. R. Petersen, R. E. Link, J. J. Braam, S. van der Zwaag, A statistical evaluation of the staircase and the ArcSin√P methods for determining the fatigue limit, *Journal of Testing and Evaluation*, 1998, **26**, 125, doi: 10.1520/jte11982j.
[37] A. Gabelli, J. Lai, T. Lund, K. Rydén, I. Strandell, G. E. Morales-Espejel, The fatigue limit of bearing steels - Part II: characterization for life rating standards, *International Journal of Fatigue*, 2012, **38**, 169-180, doi: 10.1016/j.ijfatigue.2011.12.006.
[38] E. Kerscher, K.-H. Lang, Increasing the fatigue limit of a high-strength bearing steel by a deep cryogenic treatment, *Journal of Physics*: *Conference Series*, 2010, **240**, 012059, doi: 10.1088/1742-6596/240/1/012059.
[39] S. Zhirafar, A. Rezaeian, M. Pugh, Effect of cryogenic treatment on the mechanical properties of 4340 steel, *Journal of Materials Processing Technology*, 2007, **186**, 298-303, doi: 10.1016/j.jmatprotec.2006.12.046.
[40] P. Baldissera, Fatigue scatter reduction through deep cryogenic treatment on the 18NiCrMo$_5$ carburized steel, *Materials & Design*, 2009, **30**, 3636-3642, doi: 10.1016/j.matdes.2009.02.019.

